

**FULL PAPER**

# Metabolite profiling based on UPLC-QTOF-MS/MS and evaluation of *Petiveria alliacea* leaves extract as an *in silico* anti-inflammatory

Nurmawati Fatimah<sup>a</sup>  | Arifa Mustika<sup>b,\*</sup>  | Sri Agus Sudjarwo<sup>c</sup>  | Nurul Shahfiza Noor<sup>d</sup> <sup>a</sup>Doctoral Program of Medical Science, Faculty of Medicine, Airlangga University, Surabaya, 60132, Indonesia<sup>b</sup>Department of Anatomy, Histology and Pharmacology, Faculty of Medicine, Airlangga University, Surabaya, 60132, Indonesia<sup>c</sup>Faculty of Veterinary Medicine, Airlangga University, Surabaya, 60132, Indonesia<sup>d</sup>Department of Toxicology, Advanced Medical and Dental Institute, Universiti Sains Malaysia, Bertam, 13200, Penang

Inflammation is often the key element that results in dysregulation of one or more of the biochemical pathways responsible for the pathological development of disease. Uncontrolled acute inflammation can become chronic, contributing to various chronic inflammatory diseases such as cardiovascular disease, diabetes, arthritis, and cancer. Primary stimulation is generally elicited by proinflammatory cytokines such as interleukin 1 $\beta$  (IL-1 $\beta$ ), interleukin 6 (IL-6), and tumor necrosis factor  $\alpha$  (TNF- $\alpha$ ). *Petiveria alliacea* L. has been reported pharmacologically to have anti-microbial, anti-cancer, immunomodulatory, analgesic, and anti-inflammatory activities. The purpose of this study was to determine the *Petiveria alliacea* potential as an anti-inflammatory by inhibiting proinflammatory cytokine target proteins (IL1R and TNFAR) *in silico*. The test compounds are selected compounds obtained from the UPLC-QToF-MS/MS results of *Petiveria alliacea* leaf extract and the reference results from Google, which are compounds that have been widely studied. Prior to docking, the downloaded compounds were prepared using PyRx 0.8, and then docked with both receptors using AutoDock Vina, and visualization of the docking results was carried out using Biovia Discovery Studio 2019. The docking results showed that the Myricitrin compound had a lower binding affinity value than the IL1R receptor inhibitor, which indicated that it had better activity compared to the inhibitor as well as the isoarborinol acetate compound against TNFAR. Therefore, the conclusion of this study is that the 70% ethanol extract of *Petiveria alliacea* leaves has anti-inflammatory activity by inhibiting pro-inflammatory cytokines (IL1R and TNFAR).

**\*Corresponding Author:**

Arifa Mustika

Email: [arifa-m@fk.unair.ac.id](mailto:arifa-m@fk.unair.ac.id)

Tel.: +62 87851540939

**KEYWORDS**Anti-inflammatory; chronic disease; *in silico*; metabolite profiling; *Petiveria alliacea*.**Introduction**

Inflammation is a pathogenic event arising from the immune system's activation in

response to various stimuli. Often, inflammation plays a significant role when one or more biochemical pathways

responsible for the development of inflammation-related disorders become dysregulated [1,2]. Many chronic diseases, including cancer, diabetes, rheumatoid arthritis, cardiovascular ailments, intestinal disorders, and other forms of arthritis, share inflammation as a common underlying cause [3,4].

The body creates acute inflammation as a sort of short-term inflammation to address damage, illness, and infection [2]. Nevertheless, if acute inflammation is not addressed, it can progress to chronic inflammation, contributing to many chronic inflammatory diseases [4,5]. The existence of monocytes, lymphocytes, and macrophages, as well as the connective tissue and growth of blood vessels, are the primary features of chronic inflammation. An organism's inflammatory response might eventually start to harm healthy cells, tissues, and organs while living with chronic inflammation. Internal scarring, tissue death, and DNA damage are all its possible long-term effects [2].

Intracellular signaling pathways are activated by inflammatory stimuli, and this in turn activates the synthesis of inflammatory mediators. Primary inflammatory triggers like microbial products and cytokines, such as interleukin 6 (IL-6), interleukin 1 $\beta$  (IL-1 $\beta$ ), and tumor necrosis factor  $\alpha$  (TNF- $\alpha$ ), drive inflammation through their interactions with receptors like TLRs, IL-6R, IL-1R, and TNFR. These interactions activate key cellular signaling routes, including the Janus kinase (JAK)/signal transducer and activator transcription (STAT) pathways, nuclear factor kappa B (NF- $\kappa$ B), and mitogen-activated protein kinase (MAPK) [4,6].

Guinea chicken grass, sometimes referred to as *Petiveria alliacea* L. (Phytolaccaceae), is a tropical medicinal plant. It is a perennial plant that grows wild in Central America, South America, and Africa [7]. *P. alliacea* is employed ethnopharmacologically to treat rheumatism, diabetes, and inflammation. It can also be used as a depurative, anesthetic,

sedative, antispasmodic, antihelminthic, antispasmodic, and antinociceptive agent. *P. alliacea* has been shown to possess pharmacological properties that include antimicrobial, anti-cancer, immunomodulatory, analgesic, and anti-inflammatory effects [8-10]. This study aims to determine the metabolite profiling of *P. alliacea* extracts as well as their potential as anti-inflammatory agents by *in silico* analysis of these compounds with pro-inflammatory cytokine target proteins, such as IL1R and TNFR.

## Materials and methods

### *Extraction of petiveria alliacea leaves*

*Petiveria alliacea* leaves were obtained and identified at the Unit Pelaksana Teknis (UPT) Materia Medika, Batu, East Java, Indonesia, with the identification letter of 074/349/102.7-A/2021, and then the leaves of *Petiveria alliacea* were extracted by maceration with 70% ethanol solvent in a ratio of 1:10, for 3x24 hours with occasional stirring.

### *Metabolite profiling using UPLC-QToF-MS/MS*

Metabolite profiling was conducted at the Forensic Laboratory Center for the Indonesian National Police Criminal Investigation Agency using the UPLC-QToF-MS/MS system. The extract was prepared using the solid-phase extraction (SPE) method. Subsequently, 5  $\mu$ l of each extract was introduced into the MS Xevo G2-S QToF detector, part of the ACQUITY UPLC<sup>®</sup> H-Class System (both by Waters, USA). Sample separation occurred on an ACQUITY BEH C18 column (1.7  $\mu$ m 2.1  $\times$  50 mm) with a flow rate of 0.2 ml/min, utilizing acetonitrile + 0.05% formic acid and water + 0.05% formic acid as the mobile phases. The UPLC-QToF-MS/MS analysis results were processed using the MassLynx 4.1 software, which generated chromatogram data and m/z spectra for each peak. Chemical identifications were further validated using online resources: MassBank

(<https://massbank.eu/MassBank>) and ChemSpider (<https://www.chemspider.com>) [11].

### *Ligand preparation*

The test compounds are selected compounds obtained from the UPLC-QToF-MS/MS results of *Petiveria alliacea* leaves extract and the reference results from Google, which are compounds that have been widely studied [10,12-13]. The 3D structures of the compounds in Table 1 were obtained from the PubChem database (<https://pubchem.ncbi.nlm.nih.gov/>). Compounds were prepared by optimizing their conformation using the Open Babel 2.3.1 plug-in integrated in the PyRx 0.8 software. The optimum conformation will make the ligand structure flexible [14,15]. After preparation, the compounds are stored in the Protein Data Bank (PDB) format.

### *Preparation of Inhibitor Compounds for Control*

Inhibitor compounds are compounds that have the ability to inhibit a protein. The list of inhibitors used is indicated in **Table 2**. The inhibitor compounds were prepared in the same way as the active compounds.

### *Protein Preparation*

When using the ID listed in Table 2, it is possible to download the 3D structures of the IL1R and TNFAR proteins from the RCSB PDB database (<https://www.rcsb.org/>) [16]. Using the Biovia Discovery Studio 2019 program, contaminating compounds were eliminated to prepare these proteins [17]. This is necessary because the contaminant molecules will hinder the protein binding process with the test ligand.

### *Molecular docking*

Molecular docking was carried out using AutoDock Vina, which was integrated into the

PyRx 0.8 software [18]. The selected docking result is the one with the lowest binding affinity value in each mode. The binding affinity value reflects the strength of biomolecular interaction between the ligand and the receptor, the smaller it is, the more stable it is and indicates the stronger affinity of the ligand for the receptor [19].

### *Chemical interactions*

Visualization of the docking results was carried out using the Biovia Discovery Studio 2019 software [20,21]. The chemical interactions shown are hydrogen bonds, hydrophobic interactions, electrostatic interactions, and unfavorable interactions. Interactions that produce many hydrogen bonds are considered stable [11]. This is because hydrogen bonds are the strongest of all types of bonds in molecule docking [22].

### *Structural visualization*

Visualization was performed using Discovery Studio 2019 software. Ligands and proteins are displayed in 3D structures to provide an overview of the ligands and proteins before they are interacted with [23,24]. The 3D visualization of protein-ligand interactions was carried out using whole visualization, and then focusing on the ligand-binding side of the protein using surface structures. Experiment should start as a continuation to introduction on the same page. All important materials used along with their source shall be mentioned. The main methods used shall be briefly described, with references. New methods or substantially modified methods may be described in sufficient detail. The statistical method and the chosen significance level shall be clearly stated.

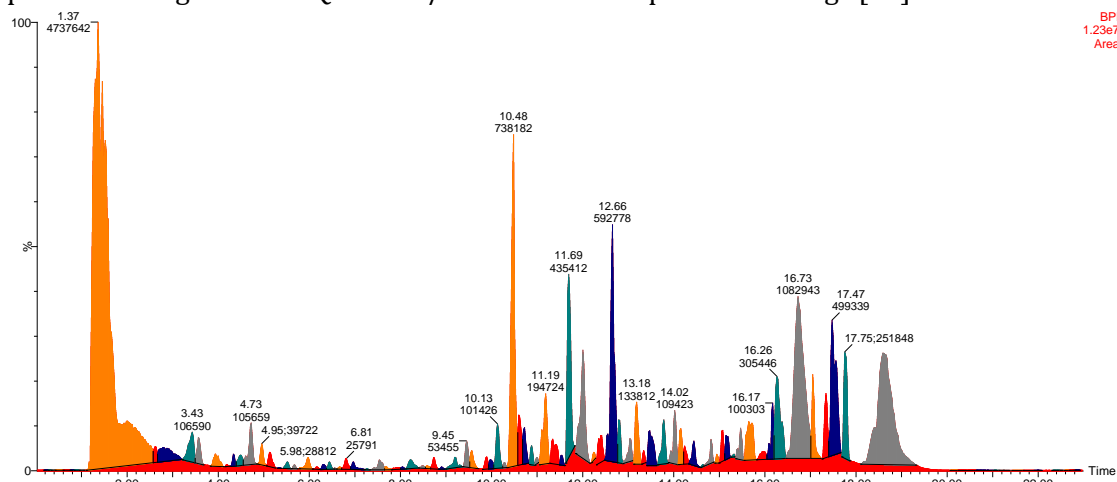
## **Results and discussion**

### *Metabolite profiling*

Metabolite profiling was conducted to determine the composition of compounds in

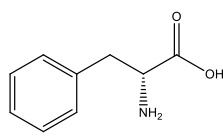
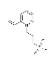
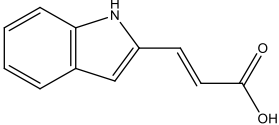
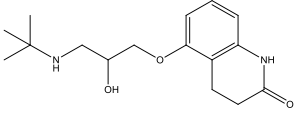
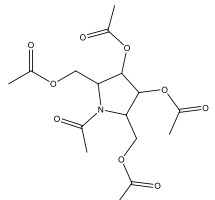
the *Petiveria alliacea* extract [25]. The extract was prepared using the Solid Phase Extraction (SPE) method before being profiled using a UPLC-QToF-MS/MS device.

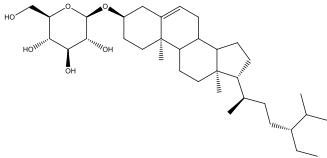
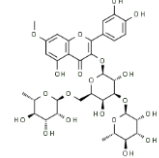
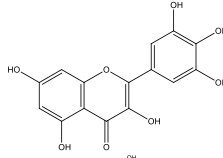
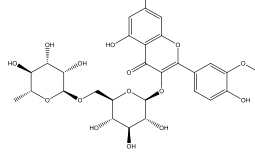
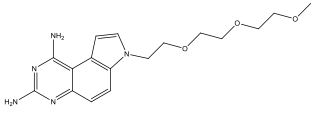
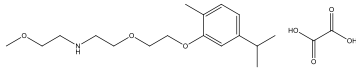
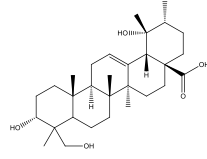
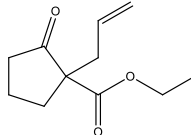
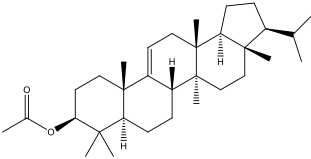
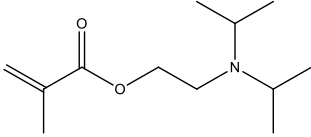
The advantage of using SPE for sample preparation is its ability to filter out impurities, enhancing the sensitivity of the spectral readings [26].

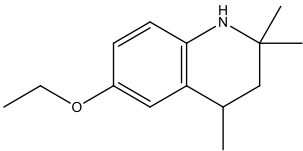
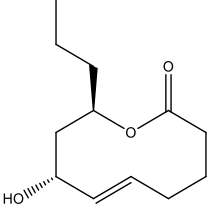
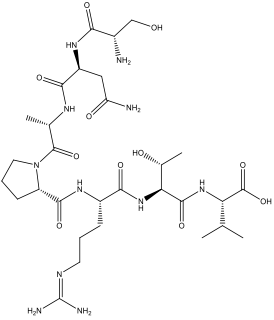
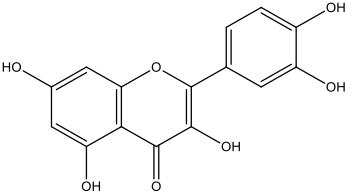
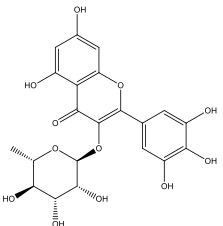
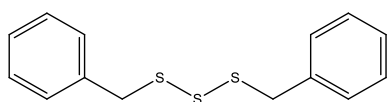
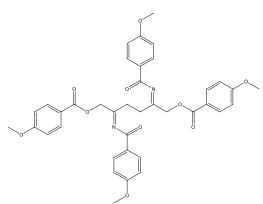
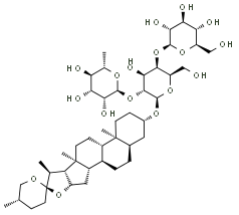



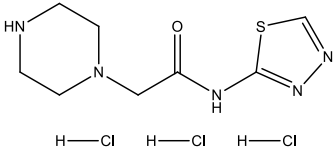
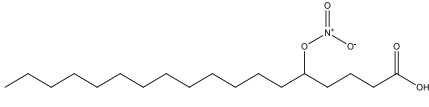
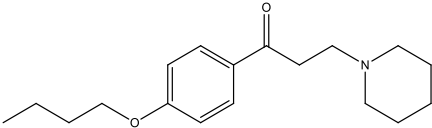
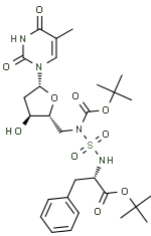
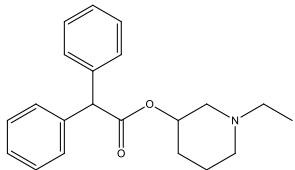
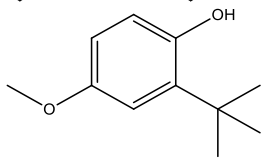
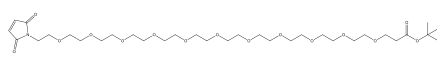
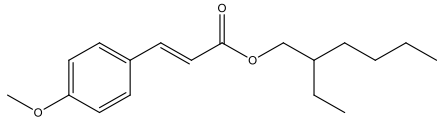
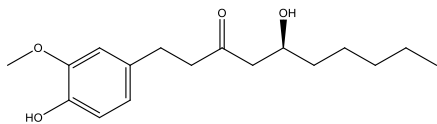
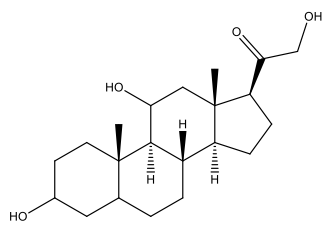
**FIGURE 1** Total ion chromatogram (TIC) of *Petiveria alliacea* leaves extract

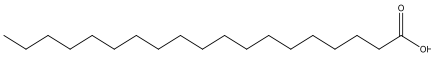
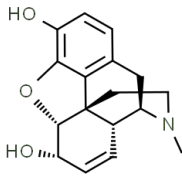
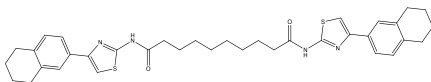
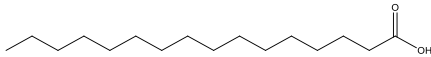
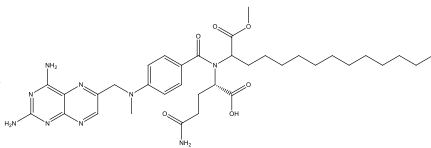
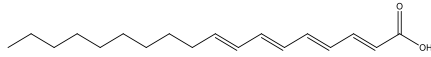
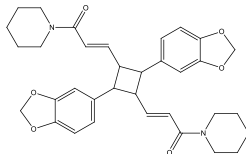
**TABLE 1** Prediction of compounds in *Petiveria alliacea* leaves extract

No.	RT	%Area	Measured Mass	Calculated Mass	Molecular Formula	Compound Name	Structure
1	2.617	0.3856%	165.0793	165.0790	C <sub>9</sub> H <sub>11</sub> NO <sub>2</sub>	D-Phenylalanine	
2	3.433	1.2318%	227.0619	227.0616	C <sub>10</sub> H <sub>13</sub> NO <sub>3</sub> S	3-(2-Vinyl-1-pyridiniumyl)-1-propanesulfonate	
3	3.567	0.7016%	187.0634	187.0634	C <sub>11</sub> H <sub>9</sub> NO <sub>2</sub>	Indoleacrylic acid	
4	3.939	0.5034%	292.1785	292.1787	C <sub>16</sub> H <sub>24</sub> N <sub>2</sub> O <sub>3</sub>	Carteolol	
5	4.199	0.0251%	373.1369	373.1373	C <sub>16</sub> H <sub>23</sub> NO <sub>9</sub>	2,5-Bis(acetoxymethyl)-1-acetyl-3,4-pyrrolidinediyl diacetate	

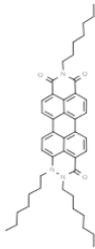
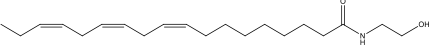
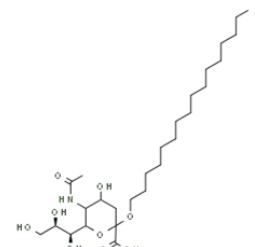
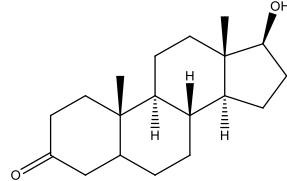
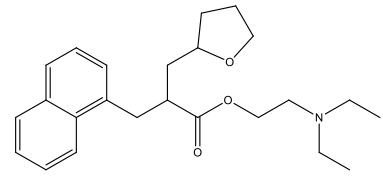
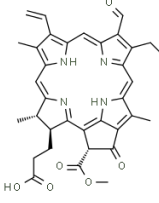
6	4.332	0.2299%	581.2687	576.8400	C35H60O6	Daucosterol	
7	4.487	0.3602%	770.2265	770.2270	C34H42O20	Xanthorhamnin B	
8	4.726	1.2210%	770.2257	770.2256	C31H34N10O14	Unknown	Unknown
9	4.952	0.4590%	316.0580	318.2300	C15H10O8	Myricetin	
10	5.127	0.4135%	624.1690	624.1691	C28H32O16	Narcisin	
11	5.324	0.0087%	345.1797	345.1801	C17H23N5O3	7-[2-[2-(2-Methoxyethoxy)ethoxy]ethyl]-7H-pyrrolo[3,2-f]quinazoline-1,3-diamine	
12	5.521	0.1570%	385.2100	385.2101	C19H31NO7	2-[2-(5-Isopropyl-2-methylphenoxy)ethoxy]-N-(2-methoxyethyl)ethanamine ethanedioate	
13	5.676	0.0643%	483.2318	488.7000	C30H48O5	Barbinervic acid	
14	5.977	0.3329%	196.1099	196.1100	C11H16O3	2-Allyl-2-carboethoxycyclopentanone	
15	6.153	0.0437%	479.2366	468.7500	C32H52O2	Isoarborinol acetate	
16	6.308	0.1265%	213.1729	213.1729	C12H23NO2	2-(Diisopropylamino)ethyl methacrylate	

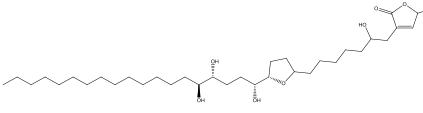
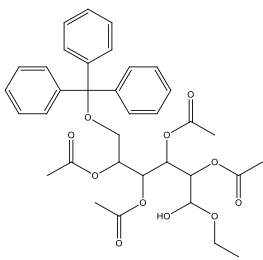
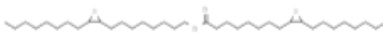
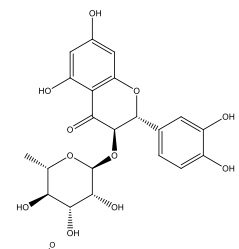
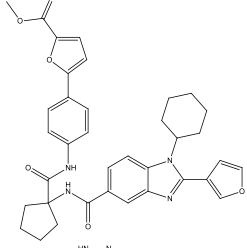
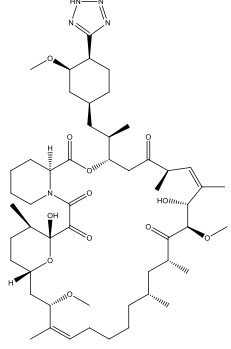
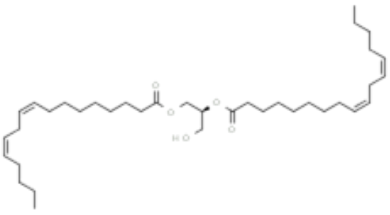
17	6.442	0.1602%	219.1623	219.1623	C14H21NO	Dihydroethoxyquin	
18	6.554	0.0091%	212.1411	212.1413	C12H20O3	Herbarumin III	
19	6.659	0.0411%	743.3922	743.3926	C30H53N11O11	L-Seryl-L-asparaginyl-L-alanyl-L-prolyl-N5-(diaminomethylene)-L-ornithyl-L-threonyl-L-valine	
20	6.814	0.2980%	313.1313	302.2400	C15H10O7	Quercetin	
21	6.969	0.2173%	476.1301	464.3800	C21H20O12	Myricitrin	
22	7.258	0.0120%	278.0948	278.4600	C14H14S3	Dibenzyl trisulphide	
23	7.538	0.3534%	684.2686	684.2683	C38H40N2O10	1,2-Ethanediybis{[(4-methoxybenzoyl)imino]-2,1-ethanediy} bis(4-methoxybenzoate)	
24	7.672	0.0691%	886.4924	886.4926	C45H74O17	Iso-terrestrosin B	
25	7.940	0.0814%	884.4749	884.4750	C32H56N26O3S	Unknown	

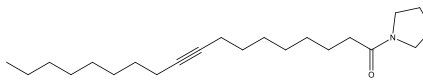
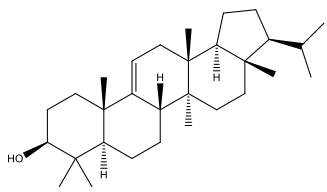
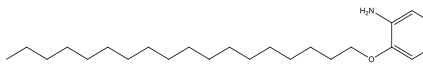
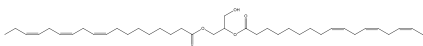
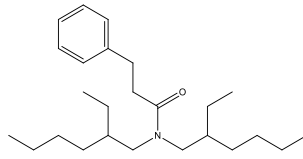
26	8.044	0.0362%	335.0142	335.0141	C8H16N5OSC13	2-(1-Piperazinyl)-N-(1,3,4-thiadiazol-2-yl)acetamide trihydrochloride	
27	8.220	0.3580%	345.2515	345.2515	C18H35NO5	5-Nitrostearic acid	
28	8.488	0.0590%	289.2039	289.2042	C18H27NO2	Dyclonine	
29	8.593	0.0661%	624.2463	624.2465	C28H40N4O10S	2-Methyl-2-propanyl (2S)-2-[[[(2R,3S,5R)-3-hydroxy-5-(5-methyl-2,4-dioxo-3,4-dihydro-1(2H)-pyrimidinyl)tetrahydro-2-furanyl)methyl]][(2-methyl-2-propanyl)oxy]carbonyl]sulfamoyl]amino]-3-phenylpropanoate	
30	8.726	0.2935%	323.1881	323.1886	C21H25NO2	1-Ethyl-3-piperidinyl diphenylacetate	
31	9.191	0.3565%	180.1152	180.1151	C11H16O2	3-BHA	
32	9.450	0.6177%	709.3884	709.3885	C33H59NO15	2-Methyl-2-propanyl 1-(2,5-dioxo-2,5-dihydro-1H-pyrrol-1-yl)-3,6,9,12,15,18,21,24,27,30,33-undecaohexatriacontan-36-oate	
33	9.563	0.4168%	290.1882	290.1882	C18H26O3	Octinoxate	
34	9.894	0.2778%	294.1831	294.1831	C17H26O4	Gingerol	
35	10.133	2.4505%	350.2458	350.2457	C21H34O4	Tetrahydrocorticosterone	

36	10.287	0.0834%	298.0480	C19H38O2	Nonadecanoic acid	
37	10.484	10.6739%	285.1367	C17H19NO3	D-(-)-Morphine	
38	10.878	0.3577%	1017.4996	C45H79NO24	Unknown	Unknown
39	10.990	0.0961%	626.2745	C36H42N4O2S2	N,N'-Bis[4-(5,6,7,8-tetrahydro-2-naphthalenyl)-1,3-thiazol-2-yl]decanediamide	
40	11.187	2.2502%	855.4464	C39H69NO19	Unknown	Unknown
41	11.539	0.1995%	265.2771	C16H32O2	Hexadecanoic acid	
42	11.693	5.0316%	693.3958	C35H51N9O6	N2-(4-{(2,4-Diamino-6-pteridyl)methyl}(methylamino)benzoyl)-N-(1-methoxy-1-oxo-2-tetradecanyl)-L-glutamine	
43	12.003	3.8440%	276.2095	C18H28O2	Octadecatetraenoic acid	
44	12.656	7.7801%	292.1785	C20H49N7O7S	Unknown	Unknown
45	12.790	1.0075%	570.2728	C34H38N2O6	Dipiperamide A	



46	13.037	0.5922%	671.4090	671.4087	C4H53N3O3	1,2,9-Triheptyl-1,2-dihydroisoquinolino[4',5':6,5,10]anthra[2,1,9-def]cinnoline-3,8,10(9H)-trione	
47	13.183	1.5463%	495.3329	495.3327	C12H37N19O3	Unknown	Unknown
48	13.338	0.2101%	321.2668	321.2668	C20H35NO2	$\alpha$ -Linolenoyl Ethanolamide	
49	13.472	1.4060%	533.3568	533.3564	C27H51NO9	Hexadecyl 5-acetamido-3,5-dideoxy-6-[(1S,2R)-1,2,3-trihydroxypropyl]hex-2-ulopyranosidonic acid	
50	13.782	1.2270%	290.2249	290.2246	C19H30O2	Androstanolone	
51	14.020	1.2645%	383.2459	383.2461	C24H33NO3	Naftidrofuryl	
52	14.154	0.8332%	509.3566	509.3564	C25H50NO9	Unknown	Unknown
53	14.238	0.3740%	606.2474	606.2479	C35H34N4O6	Pheophorbide B	
54	14.443	0.6116%	608.4434	608.4434	C31H64N2O7S	Unknown	Unknown

55	14.640	0.0257%	523.3642	523.3640	C14H41N19O3	Unknown	Unknown
56	14.815	0.4355%	596.4651	596.4652	C35H64O7	Gigantetrocin	
57	15.075	0.7670%	636.2575	636.2571	C35H40O11	1-Ethoxy-1-hydroxy-6-(trityloxy)-2,3,4,5-hexanetetrayl tetraacetate	
58	15.146	0.6232%	596.4658	596.4661	C36H68O2S2	8-(3-Octyl-2-thiiranyl)octyl 8-(3-octyl-2-thiiranyl)octanoate	
59	15.322	0.0335%	462.3710	450.3900	C21H22O11	Astilbin	
60	15.468	0.6942%	620.2635	620.2635	C36H36N4O6	Methyl 5-[4-({[1-({[1-cyclohexyl-2-(3-furyl)-1H-benzimidazol-5-yl]carbonyl}amino)cyclopentyl]carbonyl}amino)phenyl]-2-furoate	
61	15.644	1.9669%	969.6036	969.6038	C52H83N5O12	(1R,9S,12S,15R,16Z,18R,19R,21R,23R,28Z,30S,32S,35R)-1,18-Dihydroxy-19,30-dimethoxy-12-[(2R)-1-[(1S,3R,4R)-3-methoxy-4-(2H-tetrazol-5-yl)cyclohexyl]-2-propanyl]-15,17,21,23,29,35-hexamethyl-11,36-dioxo-4-azatricyclo[30.3.1.04,9]hexatriaconta-16,28-diene-2,3,10,14,20-pentone	
62	15.975	0.3623%	588.4750	588.4754	C37H64O5	(2S)-3-Hydroxy-1,2-propanediyl (9Z,12Z,9'Z,12'Z)bis(-9,12-heptadecadienoate)	

63	16.171	1.1591%	333.3031	333.3032	C22H39NO	1-(9-Octadecynoyl)pyrrolidine	
64	16.263	3.5297%	428.3657	426.7200	C30H50O	Isoarborinol	
65	16.728	12.5144%	931.6254	931.6259	C51H81N9O <sub>7</sub>	Unknown	Unknown
66	17.050	1.6483%	361.3348	361.3345	C24H43NO	2-(Octadecyloxy)aniline	
67	17.339	1.5642%	612.4758	612.4754	C39H64O5	1,2-Dilinolenin	
68	17.473	5.7703%	953.6086	953.6089	C52H83N5O11	Unknown	Unknown
69	17.753	2.9103%	373.3347	373.3345	C25H43NO	N,N-Bis(2-ethylhexyl)-3-phenylpropanamide	
70	18.590	14.1685%	791.5554	791.5553	C30H73N13O11	Unknown	Unknown

To avoid bias when identifying the sample, the total ion chromatogram (TIC) analysis of the blank was performed before the TIC of the chemicals in the sample. MassLynx 4.1 software was used to analyze the mass spectrum of each TIC peak, and the results were then verified against the ChemSpider and MassBank web databases. Figure 1 displays the total ion chromatogram (TIC) of the results of the metabolite profiling of *Petiveria alliacea* extract using the UPLC-QToF-MS/MS instrument. Table 1 presents

the % area, compound name, retention time (RT), m/z, molecular formula, and its activities as determined by literature studies. Metabolite profiling with UPLC-QToF-MS/MS showed that an extract of *Petiveria alliacea* had a total of 70 compounds, 58 of which were known and 12 of which were unknown. Not all peaks in TIC could be recognized during the metabolite profiling method based on the total number of chemicals measured. The extract from *Petiveria alliacea* contains unidentified chemicals, which is a sign of this.

Unknown compounds are substances that cannot be identified in the database, they can be impurities or degradants that are still detectable by instruments or new substances that have not yet been included in the database, particularly if they are present in large amounts [27].

Based on the analysis of these metabolites, there are a number of dominant or main compounds. These are compounds with more of them than other compounds in the sample, which is shown by the percent area. The major compounds in *Petiveria alliacea* extract are D-(-)-Morphine with an area percentage of 10.6739%; N2-(4-[[[2,4-Diamino-6pteridiny]methyl](methyl)amino]benzoyl)-N-(1-methoxy-1-oxo-2-tetradecanyl)-L-glutamine with an area percent as much as 5.0316%; and Octadecatetraenoic acid with an area percent of 3.8440%. In addition, there are also several compounds that have activity as antioxidants and anti-inflammatories, such as Isoarborinol with an area percent of

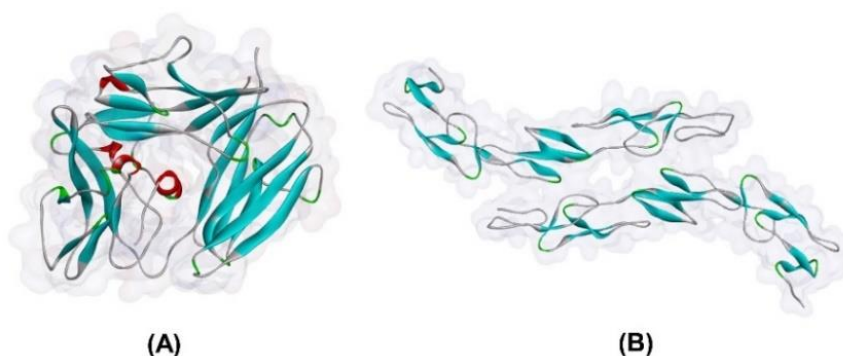
3.5927%, Myricetin with an area percent of 0.4590%, Quercetin with an area percent of 0.4590%, and so on [28-33]. This shows that *Petiveria alliacea* extract has the potential to have activity as an antioxidant and anti-inflammatory.

#### Protein Structure

The list of proteins used in this study along with their PDB ID is indicated in Table 2. The control compounds used in this analysis are also listed in Table 2. The control compounds are inhibitory compounds for each protein that have been discovered by previous researchers. The 3D structure of the protein is displayed in a ribbon style with secondary structure staining. The red color represents the helix structure, the light blue color represents the beta-sheet structure, the white color represents the loop structure, and the green color represents the coil structure (Figure 2).

**TABLE 2** Protein samples and their inhibitors

Proteins	RCSB PDB	Inhibitors	ID
IL1R	1GOY	IL1R Antagonist	10447660
TNFAR	3ALQ	Resatorvid	11703255



**FIGURE 2** 3D structure of the target protein. (A) IL1R and (B) TNFAR

#### Molecular docking

The type of chemical bond produced and the value of binding affinity have a strong

correlation with docking results. The amount of power needed to bind a protein to its ligand is called binding affinity. The easier it is for the ligand to bind to the protein and the more

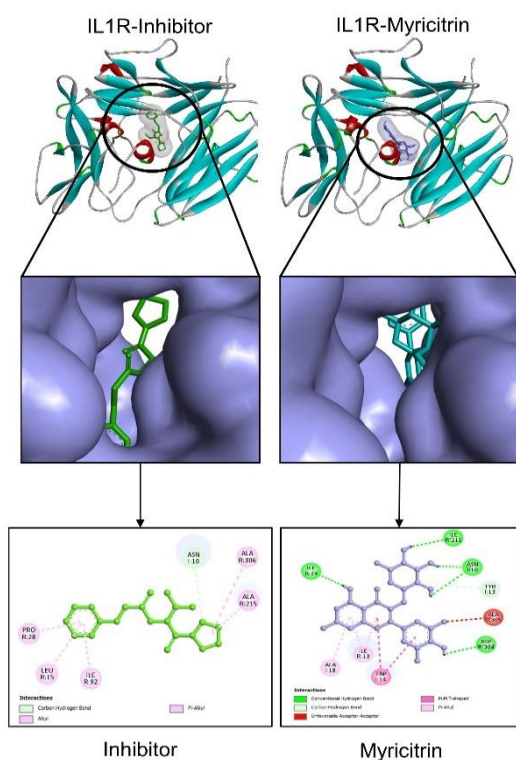
potential it has to affect the protein, the lower the binding affinity value [34]. The results of the protein-compound docking yielded binding affinity values, as provided in Table 3. From these results, it can be seen that the

IL1R-Myricitrin complex and TNFAR-Isoarborinol acetate have the most negative binding affinity values.

**TABKE 3** Binding affinity from molecular docking results

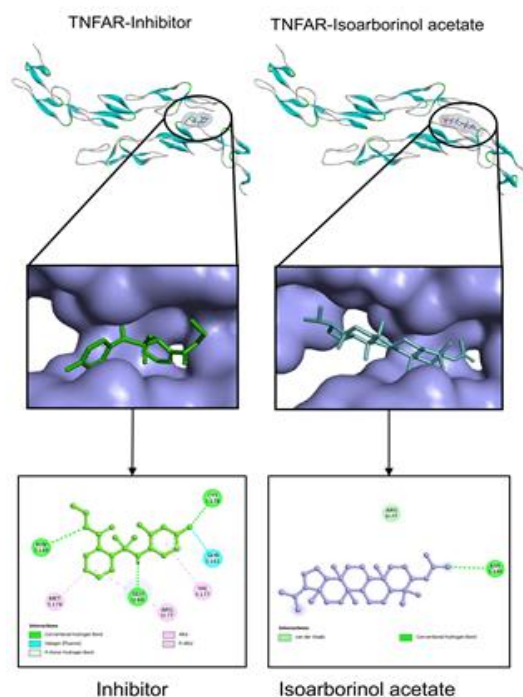
Compound	IL1R	TNFAR
Inhibitors	-8.3	-6.7
Myricetin	-8.9	-7.3
Myricitrin	-9.8	-8.0
Nonadecanoic acid	-6.3	-4.1
Quercetin	-8.9	-7.2
Astilbin	-9.3	-7.7
Barbinervic acid	-7.9	-8.1
Daucosterol	-8.9	-8.0
Dibenzyl trisulphide	-6.9	-4.9
Isoarborinol acetate	-8.3	-8.3
Hexadecanoic acid	-6.0	-4.6

Note: The green highlight mark indicates the most negative binding affinity value



**FIGURE 3** Interaction between IL1R with inhibitors and Myricitrin

Docking results between the IL1R protein and the test compounds showed the test compound with the most negative binding



**FIGURE 4** Interaction between TNFAR with Inhibitors and Isoarborinol acetate

affinity value (Figure 3). Myricitrin interacts at the same amino acid residue as the inhibitor, namely at Asn10 (Table 4). The

docking results between TNFAR and the test compounds show that all the test compounds bind on the same side as the inhibitor (Figure 4). The same binding position as the inhibitor indicates that the test compound has similar activity to the Inhibitor, namely inhibiting

TNFAR protein activity (Table 4) [35]. Isoarborinol acetate interacts with TNFAR by forming a hydrogen bond in Asn149. The residue is also the position of the inhibitor interaction on TNFAR.

**TABLE 4** Details of protein-ligand interactions with the best results

Proteins	Compound	Interaction position	
		Hydrogen bond	Hydrophobic interactions
IL1R	Inhibitors	Asn10	Pro28, Leu15, Ile92, Ala215, and Ala306
	Myricitrin	<u>Asn10</u> , Tyr13, Ile14, and Asp304	Ile13, Ile14, and Ala18
TNFAR	Inhibitors	Asn149, Glu48, and Cys178	Arg77, Met174, and Val177
	Isoarborinol acetate	<u>Asn149</u>	-

Note: The underscore (   ) indicates the same interaction position as the inhibitor.

Some of the classic cytokines that trigger the inflammatory response in general disease are IL-6, IL-1, TNF- $\alpha$ , and the IFN family, these have also been described in the pathology of diabetes, which provides clinical benefit by blocking these cytokines [36].

IL-1 is an inflammatory cytokine with numerous physiological and pathological roles that are crucial for preserving the balance between health and disease. Interleukin-1 has evolved, and mounting evidence emphasizes its significance in tying innate immunity to a wide range of disorders beyond inflammatory ones [37]. The IL-1 protein family encompasses several members: IL-1Ra, IL-18, IL-33, IL-36Ra, IL-36 $\gamma$ , IL-36 $\beta$ , IL-36 $\alpha$ , IL-37, IL-38, IL-1 $\alpha$ , and IL-1 $\beta$  [38,39]. Among these, the ones that act as receptor agonists are IL-18, IL-33, IL-36, IL-1 $\alpha$ , and IL-1 $\beta$ . Conversely, IL-36Ra, IL-38, and IL-1Ra serve as receptor antagonists. Notably, IL-37 stands out as the sole anti-inflammatory cytokine [37].

By regulating a number of innate immune functions, IL-1 is the primary regulator of inflammation [37,39]. From a historical perspective, IL-1 has various biological effects, such as serving as a leukocyte pyrogen, a fever

mediator, an endogenous leukocyte mediator, and an inducer of many acute phase response components and lymphocyte activating factor (LAF) [37]. In addition to IL-1, TNF- $\alpha$  plays a pivotal role in the inflammatory process. It has been observed that TNF- $\alpha$  boosts the expression of MHC I molecules, thereby hastening cell apoptosis [36]. In the diabetes context, IL-1 induces spurs local inflammation and b-cell apoptosis. On the other hand, TNF- $\alpha$  promotes speeds up b-cell apoptosis, dendritic cell maturation, and activates antigen-specific T cells [36]. Therefore, inhibition of inflammatory cytokines is very important in the pathology of disease development.

## Conclusion

In silico analysis, 70% ethanol extract of *Petiveria alliacea* leaves has anti-inflammatory activity by inhibiting pro-inflammatory cytokines (IL1R and TNFAR). Based on the binding affinity value, the compounds with the most potential as IL1R and TNFAR inhibitors were Myricitrin and Isoarborinol acetate, respectively.

## Acknowledgements

This research did not receive any specific grant from funding agencies in the public, commercial, or not-for-profit sectors.

## Authors' Contributions

All authors contributed to data analysis, drafting, and revising of the manuscript and agreed to be responsible for all the aspects of this work.

## Conflict of Interest

No potential conflict of interest was declared by the authors.

## Orcid:

Nurmawati Fatimah:

<https://www.orcid.org/0000-0002-9661-8934>

Arifa Mustika:

<https://www.orcid.org/0000-0001-6461-5782>

Sri Agus Sudjarwo:

<https://www.orcid.org/0000-0002-7998-7500>

Nurul Shahfiza Noor:

<https://www.orcid.org/0000-0002-5219-3081>

## References

[1] (a) L.F. García, Immune response, inflammation, the clinical spectrum of COVID-19, *Frontiers in immunology*, **2020**, *11*, 1441. [Crossref], [Google Scholar], [Publisher], (b) A. Ajala, A. Zairu, G. Shallangwa, S. Abechi, In-silico design, molecular docking and pharmacokinetics studies of some tacrine derivatives as anti-alzheimer agents: theoretical investigation, *Advanced Journal of Chemistry, Section A*, **2022**, *5*, 59-69. [Crossref], [Google Scholar], [Publisher], (c) F.R. Shakil Ahmed, M.J. Sultana, A. Sultana, M.F. Alom, Study of anti-thrombocyte activity of cassia fistula seeds extract and it's total phenolic and flavonoid content, in vitro Antioxidant and anti-inflammatory activities, *Asian Journal of Green Chemistry*, **2023**, *7*, 258-268. [Crossref], [Pdf],

[Publisher], (d) F. Akbarnejad, Dermatology benefits of punica granatum: a review of the potential benefits of punica granatum in skin disorders, *Asian Journal of Green Chemistry*, **2023**, *7*, 208-222. [Crossref], [Google Scholar], [Publisher], (e) N. Kalani, S.R. Mousavi, K. Eghbal, A. Kazeminezhad, Fifteen pearls in treating lumbar disk herniation: a narrative study, *Eurasian Journal of Science and Technology*, **2023**, *3*, 55-66. [Crossref], [Pdf], [Publisher] [2] (a) P.D. Gupta, T.J. Birdi, Development of botanicals to combat antibiotic resistance, *Journal of Ayurveda and integrative medicine*, **2017**, *8*, 266-275. [Crossref], [Google Scholar], [Publisher], (b) P.A. Kalvanagh, Y. Adyani Kalvanagh, Investigating the relationship between A/T 251 polymorphism of IL-8 gene and cancer recurrence after lumpectomy, *Eurasian Journal of Science and Technology*, **2023**, *3*, 178-189. [Crossref], [Pdf], [Publisher], (c) M. Rezaei, R. Azhough, Efficacy of diosmin on post-hemorrhoidectomy pain: a systematic review of clinical trials, *Eurasian Journal of Science and Technology*, **2023**, *3*, 141-146. [Crossref], [Pdf], [Publisher], (d) A. Saedi, S. Saedi, M.M. Ghaemi, M. Milani Fard, A review of epidemiological study of covid-19 and risk factors, *Eurasian Journal of Science and Technology*, **2022**, *2*, 224-232. [Crossref], [Pdf], [Publisher], (e) G. Sharma, S.B. Sharma, Synthetic impatiol analogues as potential cyclooxygenase-2 inhibitors: a preliminary study, *Journal of Applied Organometallic Chemistry*, **2021**, *1*, 66-75. [Crossref], [Google Scholar], [Publisher] [3] P. Libby, Inflammatory mechanisms: the molecular basis of inflammation and disease, *Nutrition reviews*, **2007**, *65*, 140-146. [Crossref], [Google Scholar], [Publisher]

- [4] L. Chen, H. Deng, H. Cui, J. Fang, Z. Zuo, J. Deng, L. Zhao, Inflammatory responses and inflammation-associated diseases in organs, *Oncotarget*, **2018**, *9*, 7204. [[Crossref](#)], [[Google Scholar](#)], [[Publisher](#)]
- [5] V. Sharma, R.K. Tiwari, S.S. Shukla, R.K. Pandey, Current and future molecular mechanism in inflammation and arthritis, *Journal of Pharmacopuncture*, **2020**, *23*, 54. [[Crossref](#)], [[Google Scholar](#)], [[Publisher](#)]
- [6] S. Kany, J.T. Vollrath, B. Relja, Cytokines in inflammatory disease, *International journal of molecular sciences*, **2019**, *20*, 6008. [[Crossref](#)], [[Google Scholar](#)], [[Publisher](#)]
- [7] A. Ochoa Pacheco, J. Marín Morán, Z. González Giro, A. Hidalgo Rodríguez, R.J. Mujawimana, K. Tamayo González, S. Sariego Frómata, In vitro antimicrobial activity of total extracts of the leaves of *Petiveria alliacea* L.(Anamu), *Brazilian Journal of Pharmaceutical Sciences*, **2013**, *49*, 241-250. [[Crossref](#)], [[Google Scholar](#)], [[Publisher](#)]
- [8] A. Mustika, N. Fatimah, G.M. Sari, The self-nanoemulsifying drug delivery system of *Petiveria alliacea* extract reduced the homeostatic model assessment-insulin resistance value, interleukin-6, and tumor necrosis factor- $\alpha$  level in diabetic rat models, *Veterinary World*, **2021**, *14*, 3229. [[Crossref](#)], [[Google Scholar](#)], [[Publisher](#)]
- [9] S. Oguntimehin, E. Ajaiyeoba, O. Ogbole, H. Dada-Adegbola, B. Oluremi, & A. Adeniji, Evaluation of selected Nigerian medicinal plants for antioxidant, antimicrobial and cytotoxic activities, *Research square*, **2021** [[Crossref](#)], [[Google Scholar](#)], [[Publisher](#)]
- [10] A.O. Olomieja, I.O. Olanrewaju, J.I. Ayo-Ajayi, G.E. Jolayemi, U.O. Daniel, R.C. Mordi, Antimicrobial and antioxidant properties of *petiveria alliacea*, *In IOP Conference Series: Earth and Environmental Science*, **2021**, *655*, 12015. [[Crossref](#)], [[Google Scholar](#)], [[Publisher](#)]
- [11] B. Ma'arif, F.A. Muslikh, D. Amalia, A. Mahardiani, L.A. Muchlasi, P. Riwanti, M. Agil, Metabolite profiling of the environmental-controlled growth of *Marsilea crenata* Presl, and its in vitro and in silico antineuroinflammatory properties, *Borneo Journal of Pharmacy*, **2022**, *5*, 209-228. [[Crossref](#)], [[Google Scholar](#)], [[Publisher](#)]
- [12]. J.F. Hernández, C.P. Urueña, T.A. Sandoval, M.C. Cifuentes, L. Formentini, J.M. Cuezva, S. Fiorentino, A cytotoxic *Petiveria alliacea* dry extract induces ATP depletion and decreases  $\beta$ -F1-ATPase expression in breast cancer cells and promotes survival in tumor-bearing mice, *Revista Brasileira de Farmacognosia*, **2017**, *27*, 306-314. [[Crossref](#)], [[Google Scholar](#)], [[Publisher](#)]
- [13] T.C. Alves, E. Rodrigues, J.H. Lago, C.M. Prado, C.E.N. Girardi, D.C. Hipólido, *Petiveria alliacea*, a plant used in Afro-Brazilian smoke rituals, triggers pulmonary inflammation in rats, *Revista Brasileira de Farmacognosia*, **2019**, *29*, 656-664. [[Crossref](#)], [[Google Scholar](#)], [[Publisher](#)]
- [14] A. Luqman, V.D. Kharisma, R.A. Ruiz, F. Gotz, In silico and in vitro study of trace amines (TA) and dopamine (DOP) interaction with human alpha 1-adrenergic receptor and the bacterial adrenergic receptor QseC, *Cell Physiol Biochem*, **2020**, *54*, 888-898. [[Crossref](#)], [[Google Scholar](#)], [[Publisher](#)]
- [15] H. Onyango, P. Odhiambo, D. Angwenyi, P. Okoth, In silico identification of new anti-SARS-CoV-2 main protease (M pro) molecules with pharmacokinetic properties from natural sources using molecular dynamics (MD) simulations and hierarchical virtual screening, *Journal of Tropical Medicine*, **2022**, 2022. [[Crossref](#)], [[Google Scholar](#)], [[Publisher](#)]
- [16]. P. Riwanti, M.S. Arifin, F.A. Muslikh, D. Amalia, I. Abada, A.P. Aditama, B. Ma'arif, Effect of *Chrysophyllum cainito* L. leaves on bone formation in vivo and in silico, *Tropical Journal of Natural Product Research*, **2021**, *5*, 260-264. [[Crossref](#)], [[Google Scholar](#)], [[Publisher](#)]
- [17] M.H. Widyananda, S.T. Wicaksono, K. Rahmawati, S. Puspitarini, S.M. Ulfa, Y.D. Jatmiko, N. Widodo, A potential anticancer mechanism of finger root (*Boesenbergia rotunda*) extracts against a breast cancer cell



- line, *Scientifica*, **2022**, 2022. [[Crossref](#)], [[Google Scholar](#)], [[Publisher](#)]
- [18] B. Ma'arif, M. Aminullah, N.L. Saidah, F.A. Muslikh, A. Rahmawati, Y.Y.A. Indrawijaya, M.M. Taek, Prediction of antiosteoporosis activity of thirty-nine phytoestrogen compounds in estrogen receptor-dependent manner through in silico approach, *Tropical Journal of Natural Product Research*, **2021**, *5*, 1727-1734. [[Crossref](#)], [[Google Scholar](#)], [[Publisher](#)]
- [19] F.A. Muslikh, R.R. Pratama, B. Ma'arif, N. Purwitasari, Studi In Silico Senyawa Flavonoid dalam Mengambat RNA-dependent RNA polymerase (RdRp) sebagai Antivirus COVID-19, *Journal of Islamic Pharmacy*, **2023**, *8*, 49-55. [[Crossref](#)], [[Google Scholar](#)], [[Publisher](#)]
- [20] B. Ma'arif, F.A. Muslikh, D.A.P. Fihuda, S. Syarifuddin, B. Fauziyah, December. Prediction of compounds from 96% ethanol extract of *Marsilea crenata* Presl, leaves in increasing estrogen receptor- $\alpha$  activation, In *Proceedings of International Pharmacy Ulul Albab Conference and Seminar (PLANAR)*, **2021**, *1*, 67-76. [[Crossref](#)], [[Google Scholar](#)], [[Publisher](#)]
- [21] B. Ma'arif, R.R. Samudra, F.A. Muslikh, T.J.D. Dewi, L.A. Muchlasi, December. Antineuroinflammatory properties of compounds from ethyl acetate fraction of *Marsilea crenata* C. Presl, against toll-like receptor 2 (3A7B) in silico, In *Proceedings of International Pharmacy Ulul Albab Conference and Seminar (PLANAR)*, **2022**, *2*, 8-20. [[Crossref](#)], [[Google Scholar](#)], [[Publisher](#)]
- [22] T.L. Wargasetia, H. Ratnawati, N. Widodo, M.H. Widyananda, Bioinformatics study of sea cucumber peptides as antibreast cancer through inhibiting the activity of overexpressed protein (EGFR, PI3K, AKT1, and CDK4), *Cancer Informatics*, **2021**, *20*, 11769351211031864. [[Crossref](#)], [[Google Scholar](#)], [[Publisher](#)]
- [23] B. Ma'arif, F.A. Muslikh, W. Anggraini, M.M. Taek, H. Laswati, M. Agil, In vitro anti-neuroinflammatory effect of genistein (4', 5, 7-trihydroxyisoflavone) on microglia HMC3 cell line, and in silico evaluation of its interaction with estrogen receptor- $\beta$ , *International Journal of Applied Pharmaceutics*, **2021**, *13*, 183-187. [[Crossref](#)], [[Google Scholar](#)], [[Publisher](#)]
- [24] B. Ma'arif, F.A. Muslikh, L.A. Najib, R.R.D. Atmaja, M.R. Dianti, December, In silico antiosteoporosis activity of 96% ethanol extract of *chrysophyllum cainito* L. leaves, In *Proceedings of International Pharmacy Ulul Albab Conference and Seminar (PLANAR)*, **2021**, *1*, 61-66. [[Crossref](#)], [[Google Scholar](#)], [[Publisher](#)]
- [25] J. Lu, A. Muhmood, W. Czekala, J. Mazurkiewicz, J. Dach, R. Dong, Untargeted metabolite profiling for screening bioactive compounds in digestate of manure under anaerobic digestion, *Water*, **2019**, *11*, 2420. [[Crossref](#)], [[Google Scholar](#)], [[Publisher](#)]
- [26] N.J. Simpson, *Solid-phase extraction: principles, techniques, and applications*, CRC press, **2000**. [[Google Scholar](#)], [[Publisher](#)]
- [27] A.P.R. Aditama, B. Ma'arif, D.M. Mirza, H. Laswati, M. Agil, In vitro and in silico analysis on the bone formation activity of N-hexane fraction of Semanggi (*Marsilea crenata* Presl.), *Systematic Reviews in Pharmacy*, **2020**, *11*, 837-849. [[Crossref](#)], [[Google Scholar](#)], [[Publisher](#)]
- [28] A.V. Anand David, R. Arulmoli, S. Parasuraman, Overviews of biological importance of quercetin: a bioactive flavonoid, *Pharmacognosy reviews*, **2016**, *10*, 84-89. [[Crossref](#)], [[Google Scholar](#)], [[Publisher](#)]
- [29] K.S. Park, Y. Chong, M.K. Kim, Myricetin: biological activity related to human health, *Appl Biol Chem*, **2016**, *59*, 259-269. [[Crossref](#)], [[Google Scholar](#)], [[Publisher](#)]
- [30] D.K. Semwal, R.B. Semwal, S. Combrinck, A. Viljoen, Myricetin: a dietary molecule with diverse biological activities, *Nutrients*, **2016**, *8*, 90. [[Crossref](#)], [[Google Scholar](#)], [[Publisher](#)]
- [31] L.M. Zavala-Ocampo, E. Aguirre-Hernández, N. Pérez-Hernández, G. Rivera, L.A. Marchat, E. Ramírez-Moreno, Antiamoebic activity of *petiveria alliacea* leaves and their main component, isoarborinol, *Journal of*

- microbiology and biotechnology*, **2017**, *27*, 1401-1408. [[Crossref](#)], [[Google Scholar](#)], [[Publisher](#)]
- [32] J.K. Kim, S.U. Park, Quercetin and its role in biological functions: an updated review, *EXCLI journal*, **2018**, *17*, 856–863. [[Crossref](#)], [[Google Scholar](#)], [[Publisher](#)]
- [33] P.T. Pham, H.P.T. Ngo, N.H. Nguyen, A.T. Do, T.Y. Vu, M.H. Nguyen, & B.H. Do, The anti-inflammatory activity of the compounds isolated from *Dichroa febrifuga* leaves, *Saudi journal of biological sciences*, **2023**, *30*, 103606. [[Crossref](#)], [[Google Scholar](#)], [[Publisher](#)]
- [34] K.A. Burkhard, F. Chen, P. Shapiro, Quantitative analysis of ERK2 interactions with substrate proteins: roles for kinase docking domains and activity in determining binding affinity, *Journal of Biological Chemistry*, **2011**, *286*, 2477-2485. [[Crossref](#)], [[Google Scholar](#)], [[Publisher](#)]
- [35] B. Ma'arif, D.A.P. Fihuda, F.A. Muslikh, S. Syarifuddin, B. Fauziah, D.P. Sari, & M. Agil, In silico study on the inhibition of TLR2 activation of the ethanol extract of *Marsilea crenata* Presl. Leaves, *Tumbuhan Obat Indonesia*, **2022**, *15*, 31-40. [[Google Scholar](#)], [[Publisher](#)]
- [36] J. Lu, J. Liu, L. Li, Y. Lan, Y. Liang, Cytokines in type 1 diabetes: mechanisms of action and immunotherapeutic targets, *Clinical & translational immunology*, **2020**, *9*, 1122. [[Crossref](#)], [[Google Scholar](#)], [[Publisher](#)]
- [37] N. Kaneko, M. Kurata, T. Yamamoto, et al. The role of interleukin-1 in general pathology, *Inflammation and regeneration*, **2019**, *39*, 1-16. [[Crossref](#)], [[Google Scholar](#)], [[Publisher](#)]
- [38] C. Dinarello, W. Arend, J. Sims, D. Smith, H. Blumberg, L. O'Neill, C. Gabel, IL-1 family nomenclature, *Nature immunology*, **2010**, *11*, 973-973. [[Crossref](#)], [[Google Scholar](#)], [[Publisher](#)]
- [39] A. Mantovani, C.A. Dinarello, M. Molgora, & C. Garlanda, Interleukin-1 and related cytokines in the regulation of inflammation and immunity, *Immunity*, **2019**, *50*, 778-795. [[Crossref](#)], [[Google Scholar](#)], [[Publisher](#)]

**How to cite this article:** Nurmawati Fatimah, Arifa Mustika\*, Sri Agus Sudjarwo, Nurul Shahfiza Noor, Metabolite profiling based on UPLC-QTOF-MS/MS and evaluation of petiveria alliacea leaves extract as an in silico anti-inflammatory. *Journal of Medicinal and Pharmaceutical Chemistry Research*, 2024, 6(3), 344-361. **Link:** [http://jmpcr.samipubco.com/article\\_185013.html](http://jmpcr.samipubco.com/article_185013.html)